

# Directional subset simulation method for reliability analysis

Oindrila Kanjilal<sup>[0000-0003-1855-7483]</sup> and Julien Bect<sup>[0000-0002-0867-0215]</sup>

**Abstract** Estimating the probabilities of rare failure events is a key challenge in the reliability analysis of physical systems. Subset simulation (SS) is a very popular adaptive Monte Carlo method for this problem. In SS, the small failure probability is evaluated as a product of larger conditional probabilities by iteratively sampling a sequence of nested sub-domains of the parameter space, encompassing the target failure domain of interest, using Markov chain Monte Carlo methods. For failure domains with multiple modes, the Markov chain samples used to explore the intermediate levels of SS can be trapped in a confined region of the input parameter space, leading to inaccurate failure probability estimates. In this contribution, we propose the directional subset simulation (dSS) method for this problem, which uses concepts from directional sampling to informedly propagate samples towards failure. This is accomplished through a novel selection of the intermediate failure domains, which preserves samples in several directions in the parameter space in each intermediate level. The merits of the dSS method are illustrated through a selection of numerical examples.

## 1 Introduction

One of the main goals of the condition assessment of engineering systems is to determine the safety level, or reliability, by accounting for the impact of uncertainties on system performance. These uncertainties arise from various sources, including loading, material properties, geometry and deterioration parameters. Computational reliability analysis focuses on evaluating the probability of failure:

---

Oindrila Kanjilal  
Georg Nemetschek Institute, Technical University of Munich  
80333 Munich, Germany. e-mail: [oindrila.kanjilal@tum.de](mailto:oindrila.kanjilal@tum.de)

Julien Bect  
Université Paris-Saclay, CNRS, CentraleSupélec, Laboratoire des signaux et systèmes  
91190 Gif-sur-Yvette, France. e-mail: [julien.bect@centralesupelec.fr](mailto:julien.bect@centralesupelec.fr)

$$\pi_F = \mathbf{P}(\Theta \in F) = \mathbf{P}(g(\Theta) \leq 0) = \int_{\mathbb{S}} \mathbb{1}_F(\theta) p(\theta) d\theta, \quad (1)$$

where  $\Theta$  is an  $n$ -dimensional random vector of uncertain quantities, taking values in some set  $\mathbb{S} \subseteq \mathbb{R}^n$ ,  $p$  its probability density function (PDF),  $g : \mathbb{S} \rightarrow \mathbb{R}$  the limit-state function (LSF) and  $F = \{\theta \in \mathbb{S} \mid g(\theta) \leq 0\}$  the failure domain. To simplify notations, we will identify in this article a subset  $A \subset \mathbb{S}$  with the event  $\{\Theta \in A\}$ , writing for instance  $\pi_F = \mathbf{P}(F)$  instead of  $\pi_F = \mathbf{P}(\Theta \in F)$  as in (1).

In practical applications, the failure domain may have a complex geometry, making the evaluation of the reliability integral challenging. A prominent challenge arises when the truncated PDF  $p(\theta|F) \propto p(\theta)\mathbb{1}_F(\theta)$  has multiple dominant regions, or *modes*, in the parameter space  $\mathbb{S}$ . This situation occurs in system reliability analysis problems, where failure can be due to a single component of the system subjected to multiple failure mechanisms (e.g., stress and displacement in a component), or due to simultaneous failure of multiple components. To understand failure behavior in such settings, it is important not only to compute the global failure probability  $\pi_F$ , but also to estimate the relative contribution of each mode to the failure event. Effective reliability analysis therefore requires methods that adequately explore all failure modes, which is difficult when the modes are separated by regions of low probability density.

A simple but versatile method for solving reliability problems with multi-modal failure domains is Monte Carlo simulation (MCS), which uses an independent and identically distributed (i.i.d) sample drawn from  $p$ :

$$\hat{\pi}_F^{\text{MCS}} = \frac{1}{N} \sum_{i=1}^N \mathbb{1}_F(\theta^{(i)}), \quad \theta^{(i)} \stackrel{\text{i.i.d}}{\sim} p(\theta). \quad (2)$$

This method yields an unbiased estimator of  $\pi_F$ , with coefficient of variation (CoV)  $\delta_{\text{MCS}} \approx 1/\sqrt{N\pi_F}$ . Its main drawback is the large sample size  $N$  that is required to explore the failure domain when the failure probability is small.

Analytical methods based on the FORM/SORM principle (see, e.g., [2] and references therein) do not handle “natively” problems with multiple failure mode—since they rely on an approximation of the LSF around the most probable failure point—but can be extended to work with several design points [10, 23]. A widely adopted approach for estimating small failure probabilities is to use advanced Monte Carlo methods. These methods modify the brute-force procedure with specialized techniques to sample from the important regions of a rare failure domain in a probabilistically correct and efficient way. Several advanced simulations methods have been proposed over the past decades, which can be broadly grouped as importance sampling (IS) methods [11, 16, 22], subset simulation [1] and its variants [8, 9], line sampling methods [17, 14] and directional simulation [5, 13, 24], among others. Discussions on the strengths and limitations of the different approaches for reliability analysis as well as insight on the relative performance is available in [21, 20].

In this paper, we focus on the widely used subset simulation (SS) method [1]. The key idea in SS is to introduce a nested sequence of intermediate failure domains, or *subsets*, such that the small failure probability can be decomposed into a product of

larger conditional probabilities. The probabilities are estimated by sampling from the conditional PDFs using Markov chain Monte Carlo (MCMC) [7]. SS preserves the versatility of brute-force MCS as it does not require any prior information about the system behavior and is universally applicable to all system types. However, it is well known that for certain geometries of the LSF [3], e.g., when there are sudden sharp changes in the LSF values or discontinuity in the failure domain, the Markov chains in an intermediate subset can get trapped in a confined region of the parameter space causing the modes of the subsequent conditional PDFs to remain unexplored, see Fig. 2a for an illustration. This can cause several important regions of the target failure domain to go undetected during reliability analysis, resulting in underestimation of the failure probability and (or) high sampling variance. Various enhancements of the original SS method have been proposed to overcome this weakness [19, 18, 9].

In this paper, we propose a new framework for subset simulation, which we name directional subset simulation (dSS). In dSS, the key idea is to direct the Markov samples towards the important failure regions by partitioning the parameter space into a set of communicating bins, and individually exploring each bin with suitable subsets. The subsets define a set of local intermediate failure domains in each bin and are constructed such that the global conditional failure probability over the parameter space adheres to an prescribed large value. MCS is used to allocate an initial population of samples in each bin, which are propagated to the failure domain by sequentially sampling the subsets using global MCMC moves.

The paper is organized as follows. In the next section, we briefly summarize the conventional SS method. This is followed by the description of the proposed dSS method in Section 3. In Section 4 we demonstrate the performance of the dSS method on two numerical examples. Finally, we present the conclusions in Section 5 and provide directions for future research.

## 2 Subset simulation method

Consider a failure event  $F = \{\boldsymbol{\theta} \in \mathbb{S} \mid g(\boldsymbol{\theta}) \leq 0\}$ . Let  $\infty = \gamma_0 > \gamma_1 > \gamma_2 > \dots > \gamma_T = 0$  be a decreasing sequence of thresholds, which defines a decreasing sequence

$$\mathbb{S} = F_0 \supset F_1 \supset F_2 \supset \dots \supset F_T = F \quad (3)$$

of subsets, where  $F_t = \{\boldsymbol{\theta} \in \mathbb{S} \mid g(\boldsymbol{\theta}) \leq \gamma_t\}$ ,  $0 \leq t \leq T$ . Since  $F_t \subset F_{t-1}$ , we have

$$P(F_t) = P(F_t|F_{t-1})P(F_{t-1}), \quad 1 \leq t \leq T. \quad (4)$$

Since  $P(F_0) = 1$ , the target failure probability can be expressed as  $\pi_F = \prod_{t=1}^T p_t$ , with  $p_t := P(F_t|F_{t-1}) = \int_{\mathbb{S}} \mathbb{1}_{F_t}(\boldsymbol{\theta}) f_{t-1}(\boldsymbol{\theta}) d\boldsymbol{\theta}$ , where  $f_{t-1}$  is the truncated density

$$f_{t-1}(\boldsymbol{\theta}) = \frac{\mathbb{1}_{F_{t-1}}(\boldsymbol{\theta}) p(\boldsymbol{\theta})}{\int_{\boldsymbol{\theta} \in \mathbb{S}} \mathbb{1}_{F_{t-1}}(\boldsymbol{\theta}) p(\boldsymbol{\theta}) d\boldsymbol{\theta}}. \quad (5)$$

The central idea in SS is then to estimate  $\pi_F$  by estimating the conditional failure probabilities  $p_t$ ,  $1 \leq t \leq T$ , expecting efficiency gain when these probabilities are not small. There are two key challenges in implementing this idea.

First, estimating the conditional probabilities by simulation requires the efficient generation of samples from the truncated densities  $f_t$ ,  $1 \leq t \leq T - 1$ , which in general is not trivial. This issue is resolved by using Markov chain Monte Carlo [15], in a sequential Monte Carlo [4] framework: the samples that belong to the failure domain  $F_t$  at level  $t$  form the seeds for MCMC sampling at the next level.

Second, the intermediate thresholds  $\gamma_t$ ,  $1 \leq t \leq T - 1$ , must be selected such that the  $p_t$ s are neither too small (to avoid ending up with a rare event estimation problem at each subset) nor too large (otherwise the method would require a large value of  $T$ ). To achieve this goal, the intermediate thresholds are chosen adaptively, in such a way that estimated conditional failure probabilities  $p_t$ ,  $1 \leq t \leq T - 1$ , are all equal to a given value  $\rho \in [0.1, 0.3]$  [25]. In other words,  $\gamma_t$  is the quantile of order  $\rho$  of the LSF values  $g(\boldsymbol{\theta}_{t-1}^{(i)})$ , where  $\boldsymbol{\theta}_{t-1}^{(i)}$ ,  $1 \leq i \leq N$ , are the samples generated at level  $t - 1$ . The procedure is repeated until the estimated  $\rho$ -percentile becomes negative, at which stage we have  $\gamma_T = 0$  and  $F_T = F$ . An estimate of the probability of failure is then obtained as

$$\hat{\pi}_F^{\text{SS}} = \rho^{T-1} \hat{p}_T, \quad (6)$$

where  $\hat{p}_T = \frac{1}{N} \sum_{i=1}^N \mathbb{1}_F(\boldsymbol{\theta}_{T-1}^{(i)})$ . The statistical properties of the estimator  $\hat{\pi}_F^{\text{SS}}$  have been discussed in [1, 4].

### 3 Directional subset simulation

**Main idea: more flexible intermediate failure sets.** Assume without loss of generality that  $\mathbb{S} = \mathbb{R}^n$  and  $\boldsymbol{\Theta} = (\Theta_1, \dots, \Theta_n)$  is an  $n$ -dimensional standard Gaussian random vector, i.e.,  $p(\boldsymbol{\theta}) = \prod_{i=1}^n \phi(\theta_i)$ , where  $\phi$  is the PDF of a standard Gaussian random variable. (When the parameters are not Gaussian or not independent,  $\boldsymbol{\theta}$  can be turned into a standard Gaussian random vector by means of a suitable iso-probabilistic transformation [12].)

Let  $(B_j)_{1 \leq j \leq J}$  denote a partition of the parameter space  $\mathbb{S}$ , where each subset  $B_j$ , hereafter called a *bin*, corresponds to a set of half-lines emanating from the origin and stretching outwards to infinity (i.e., a linear cone in  $\mathbb{R}^n$ ). In other words, each bin correspond to a set of *directions*. We consider for now that the bins are preselected before reliability estimation. We will propose a modified subset simulation algorithm, called directional subset simulation (dSS), which will ensure that each bin is properly explored.

Consider a particular bin  $B_j$ . For a decreasing sequence of threshold levels  $\infty = \gamma_{0,j} > \gamma_{1,j} \geq \gamma_{2,j} \geq \dots$ , the corresponding sub-domains

$$\Gamma_{t,j} = \{\boldsymbol{\theta} \in B_j \mid g(\boldsymbol{\theta}) \leq \gamma_{t,j}\}. \quad (7)$$

form a nested sequence of subsets of  $B_j$ , where  $\Gamma_{0,j} = B_j$  and  $\Gamma_{0,j} \supset \Gamma_{1,j} \supset \Gamma_{2,j} \supset \dots$ . In the proposed dSS method, we define intermediate failure domains by

$$F_t = \{\boldsymbol{\theta} \in \mathbb{S} \mid g(\boldsymbol{\theta}) \leq \gamma_t(\boldsymbol{\theta})\}, \quad (8)$$

where the  $\boldsymbol{\theta}$ -dependent thresholds  $\gamma_t$  are bin-wise constant:  $\gamma_t(\boldsymbol{\theta}) = \sum_{j=1}^J \gamma_{t,j} \mathbb{1}_{B_j}(\boldsymbol{\theta})$ . The sets  $\Gamma_{t,j}$ ,  $1 \leq j \leq J$  form a partition of  $F_t$ , and the intermediate failure domains form a decreasing sequence:  $\mathbb{S} = F_0 \supset \dots \supset F_t \supset F_{t+1} \supset \dots$  as in (3).

It can be readily seen that SS is a special case of the proposed dSS algorithm, where there is only one bin. The proposed framework introduces more flexibility in the choice of the intermediate failure domains: the inclusion of multiple thresholds at each level will make it possible to ensure, through a careful choice of the local thresholds  $\gamma_{t,j}$ , that each bin remains populated (with high probability), and is thus properly explored.

**Entering the failure domain.** In each bin the limit state  $\{g = 0\}$  will be reached at a different level, if it is reached at all: we denote by  $T_j$  the last level  $t$  such that  $\gamma_{t,j} > 0$ , with  $T_j = \infty$  if  $\gamma_{t,j} > 0$  for all  $t$ , and we set  $\gamma_{t,j} = 0$  for all  $t > T_j$ . The sequence of local thresholds in the bin  $B_j$  thus has the form (assuming  $T_j < +\infty$ ):

$$\infty = \gamma_{0,j} > \gamma_{1,j} > \dots > \gamma_{T_j,j} > \gamma_{T_j+1,j} = \gamma_{T_j+2,j} = \dots = 0.$$

Let  $\mathcal{J}_t \subseteq \{1, \dots, J\}$  be the set of all bin indices such that  $\gamma_{t,j} = 0$ . When  $\mathcal{J}_t \neq \emptyset$ , i.e., when the limit state has been reached in some bins, the dSS algorithm stops exploring these bins and focuses on the remaining bins  $B_j$ ,  $j \notin \mathcal{J}_t$ . Accordingly, we define the following intermediate sampling regions:

$$F'_t = \cup_{j \notin \mathcal{J}_t} \Gamma_{t,j},$$

which form again a decreasing sequence:  $\mathbb{S} = F'_0 \supset \dots \supset F'_t \supset F'_{t+1} \supset \dots$ . Note however that  $F'_t \not\supseteq F$  since the bins where  $\gamma_{t,j} = 0$  have been removed.

**Sampling from the truncated densities.** The dSS algorithm constructs at each level  $t$  an  $N$ -sample of (correlated) particles (approximately) distributed according to the truncated densities  $f_t \propto \mathbb{1}_{F'_t} p$ , using the particles from level  $t-1$  in a sequential Monte Carlo framework exactly as in SS (see Section 2).

Let  $M_t$  denote the number of particles from level  $t-1$  that belong to  $F'_t$ . Classical SS constructs an  $N$ -sample at stage  $t$  using  $\rho^{-1}$  steps of an MCMC chain started from each of these particles (called *seeds*), which is possible because  $M_t = N\rho$  by construction, and  $\rho^{-1}$  is an integer. In dSS, as a consequence of the selection of local thresholds (see below),  $M_t$  will typically be close, but not equal, to  $N\rho$ . To restore a population of size  $N$ , we use residual resampling [6] to determine the (random) number of particles produced by MCMC from each seed. (Note that, in the situation where  $M_t = N\rho$  and  $\rho^{-1}$  is an integer, residual resampling is equivalent to the original subset simulation approach, which is to take  $\rho^{-1}$  steps from each seed.)

**Selection of the sequence of thresholds.** We propose to select the local thresholds  $\gamma_{t,j}$  in a manner analogous to SS. More precisely, let  $N_{t,j}$  be the number of particles in bin  $B_j$  at level  $t$ ,  $j \notin \mathcal{J}_t$ , and let  $\boldsymbol{\theta}_{t,j}^{(i)} \in \Gamma_{t,j}$ ,  $1 \leq i \leq N_{t,j}$ , be the corresponding particles. These particles are (approximately) distributed according

to the truncated density  $f_{t,j} \propto \mathbb{1}_{\Gamma_{t,j}} p$ . Then, the next local threshold  $\gamma_{t+1,j}$  in bin  $B_j$  is taken equal to an estimate of the quantile of order  $\rho$  of the LSF values  $g(\boldsymbol{\theta}_{t,j}^{(i)})$ ,  $1 \leq i \leq N_{t,j}$ , if this estimate is positive, and to zero otherwise. (Since the number of samples  $N_{t,j}$  in each bin is not necessarily an integer multiple of  $\rho^{-1}$  as in SS, we use a quantile estimator based on an interpolation of the empirical cumulative distribution function.)

**Probability estimation and stopping condition.** Our goal is to estimate the probability of failure  $\pi_j = \mathbb{P}(F \cap B_j)$  in each bin  $B_j$ , and the total probability of failure  $\pi_F = \mathbb{P}(F) = \sum_{j=1}^J \pi_j$ . At level  $t$ , we have  $\gamma_{t+1,j} = 0$  for  $j \in \mathcal{J}_{t+1}$ , and therefore  $T_j \leq t$ . Thus, the probability of failure  $\pi_j$  can be decomposed for these bins as

$$\pi_j = \mathbb{P}(B_j) \prod_{t=0}^{T_j} \mathbb{P}(\Gamma_{t+1,j} | \Gamma_{t,j}) = \prod_{t=0}^{T_j+1} p_{t,j},$$

where  $p_{0,j} = \mathbb{P}(B_j) = \int_{\boldsymbol{\theta} \in \mathbb{S}} \mathbb{1}_{B_j}(\boldsymbol{\theta}) p(\boldsymbol{\theta}) d\boldsymbol{\theta}$  and  $p_{t,j} = \mathbb{P}(\Gamma_{t,j} | \Gamma_{t-1,j})$  for  $t \geq 1$ , and we have the estimate

$$\hat{\pi}_j = \prod_{t=0}^{T_j+1} \hat{p}_{t,j} = p_{0,j} \rho^{T_j} \hat{p}_{T_j+1,j}, \quad (9)$$

where  $\hat{p}_{t,j} = \rho$  for  $1 \leq t \leq T_j$ , and  $\hat{p}_{T_j+1,j} = \frac{1}{N_{t,j}} \sum_{i=1}^{N_{t,j}} \mathbb{1}_F(\boldsymbol{\theta}_{t,j}^{(i)})$ . The bin probabilities  $p_{0,j}$ ,  $1 \leq j \leq J$ , are assumed to be known—they will be equal to  $1/J$  in our numerical experiments.

For the remaining bins ( $j \notin \mathcal{J}_{t+1}$  at level  $t$ ), we are not yet in a position to estimate the probability  $\pi_j$  accurately, but we can already estimate an upper-bound, using the fact that  $T_j \geq t+1$ :

$$\hat{\pi}_{t,j}^+ = \prod_{t=0}^{t+1} p_{0,j} \rho^{t+1}.$$

We stop the algorithm when  $\sum_{j \notin \mathcal{J}_{t+1}} \hat{\pi}_{t,j}^+ \leq \varepsilon_{\text{tol}} \sum_{j \in \mathcal{J}_{t+1}} \hat{\pi}_j$ , and define our final estimate as  $\hat{\pi}_F = \sum_{j \in \mathcal{J}_{t+1}} \hat{\pi}_j$ . (We take  $\varepsilon_{\text{tol}} = 0.001$  in the numerical experiments.)

*Remark 1* Note that such a stopping criterion is possible because all the bins are explored simultaneously, rather than sequentially, as would be the case in a straightforward combination of subset simulation with stratified sampling.

## 4 Numerical examples

### 4.1 Piecewise linear function

We first consider the problem mentioned in Section 2. The LSF is given by

$$g(\theta_1, \theta_2) = \min(g_1, g_2) \quad (10)$$

where

$$\begin{aligned}
g_1(\theta_1, \theta_2) &= \begin{cases} 4 - \theta_1 & \text{for } \theta_1 > 3.5, \\ 0.85 - 0.1\theta_1 & \text{for } \theta_1 \leq 3.5, \end{cases} \\
g_2(\theta_1, \theta_2) &= \begin{cases} 0.5 - 0.1\theta_2 & \text{for } \theta_2 > 2, \\ 2.3 - \theta_2 & \text{for } \theta_2 \leq 2. \end{cases}
\end{aligned} \tag{11}$$

Here  $\theta_1$  and  $\theta_2$  are both standard Gaussian random variables. Fig. 1 depicts the contour plot of the LSF. The region to the right of the line  $\theta_1 = 4$  is the domain of the dominant failure mode  $\{g_1(\theta_1, \theta_2) \leq 0\}$  of this series system. The function values  $g_2(\theta_1, \theta_2)$  decrease rapidly in comparison to  $g_1(\theta_1, \theta_2)$  in the region near the origin. This leads to an initial steep decreasing gradient of the LSF in the direction of the secondary failure mode  $\{g_2(\theta_1, \theta_2) \leq 0\}$ , as indicated by the contour lines of the LSF in Fig. 1.

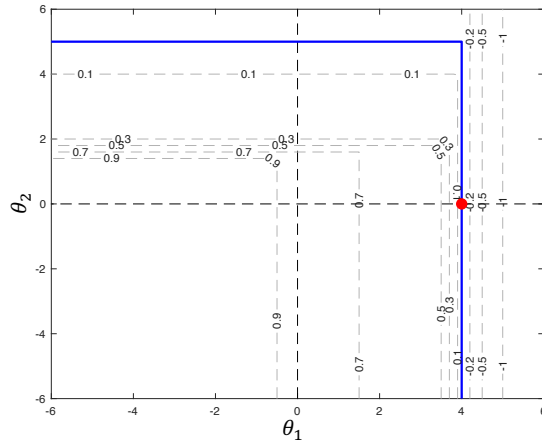


Fig. 1: Contour plot of the piecewise linear function in Example 4.1. The blue line denotes the boundary of the failure domain. The red dot is the global design point ( $\theta_1 = 4, \theta_2 = 0$ ).

To implement the dSS method, we partition the parameter space into two bins  $B_1$  and  $B_2$  of equal probability. We consider three cases:

1.  $B_1 = \left\{ (\theta_1, \theta_2) : \tan^{-1} \left( \frac{\theta_2}{\theta_1} \right) \in [-\pi + 0.8, 0.8] \right\}$  and  $B_2 = \overline{B_1}$ .
2.  $B_1 = \{(\theta_1, \theta_2) : \theta_2 < 0\}$  and  $B_2 = \{(\theta_1, \theta_2) : \theta_2 > 0\}$ .
3.  $B_1 = \{(\theta_1, \theta_2) : \theta_1 < 0\}$  and  $B_2 = \{(\theta_1, \theta_2) : \theta_1 > 0\}$ .

Figs. 2a and 2b, respectively, show the progression of the samples in the intermediate levels of the standard SS and the proposed dSS method with binning corresponding to Case 1. From the second level onward, all samples in SS move towards the secondary mode due to the steep decreasing gradient of the LSF in that direction, and the region on the right towards the dominant mode gets lost from exploration. Consequently, the samples in the final level of SS are spread out only in the

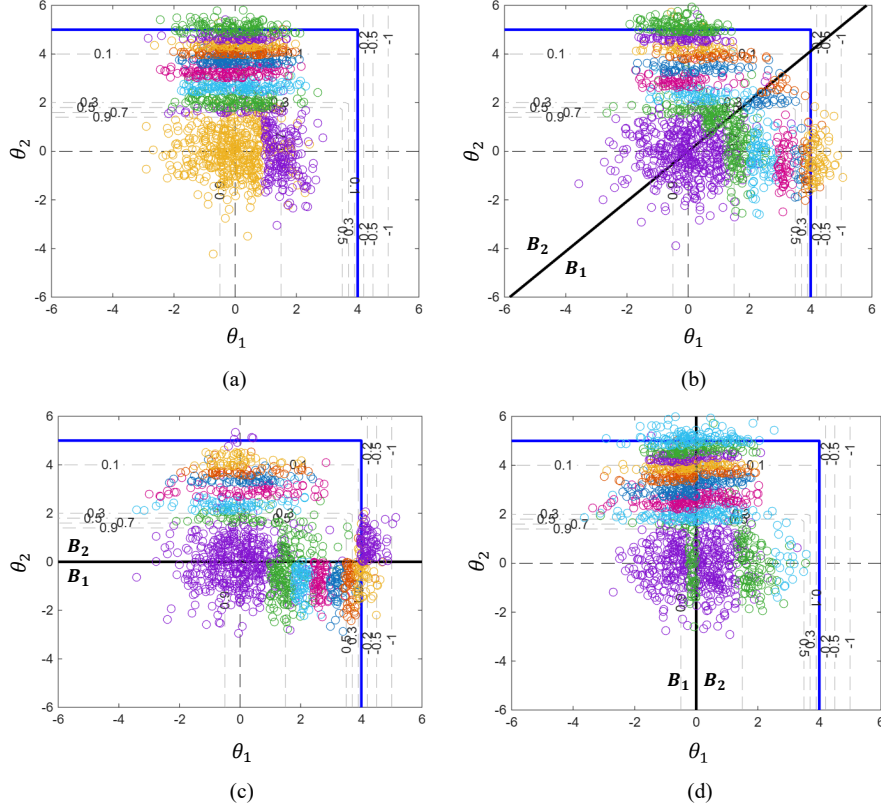


Fig. 2: Progression of samples in a typical run of (a) SS and (b–d) Case 1–3 of the dSS method for the piecewise linear LSF in Example 4.1, with  $N = 500$  samples per level and level probability of  $\rho = 0.2$ . The black line in (b–c) represent the bins used by dSS.

region of the secondary mode at the top, which causes a severe underestimation of the failure probability. In contrast, we see that both failure modes remain populated in all the intermediate levels of the dSS method, and the samples in the final level provide a complete representation of the failure domain of the series system.

Table 1 provides a quantitative comparison of the SS and the dSS methods in terms of the statistics of the estimates of  $\pi_F$  and the average number of LSF evaluations, denoted by  $N_T$ . The reference value of the probability of failure obtained from brute-force Monte Carlo simulation with  $10^8$  LSF evaluations is  $\hat{\pi}_{F,\text{ref}} = 3.19 \cdot 10^{-5}$ .  $E[\hat{\pi}_F]$  and  $\hat{\delta}_{\hat{\pi}_F}$ , respectively, denote the mean and the coefficient of variation of the sample estimates of  $\pi_F$  and the metric  $R$ , given by

$$R = \sqrt{\frac{1}{m} \sum_{i=1}^m \left( \log_{10} \left( \frac{\hat{\pi}_F^{(i)}}{\hat{\pi}_{F,\text{ref}}} \right) \right)^2},$$

Table 1: Probability of failure estimates for the piecewise linear LSF in Example 4.1, obtained from  $m = 10^4$  independent runs of each algorithm. The reference value of the probability of failure obtained from brute-force Monte Carlo simulation with  $10^8$  LSF evaluations is  $\hat{\pi}_{F,\text{ref}} = 3.19 \cdot 10^{-5}$ .

	SS				dSS (Case 1)			
	$\overline{E[\hat{\pi}_F]}$	$\hat{\delta}_{\hat{\pi}_F}$	$R$	$N_T$	$\overline{E[\hat{\pi}_F]}$	$\hat{\delta}_{\hat{\pi}_F}$	$R$	$N_T$
$N = 250$	$3.46 \cdot 10^{-5}$	4.07	2.14	2386	$4.00 \cdot 10^{-5}$	2.50	0.79	2457
$N = 500$	$3.23 \cdot 10^{-5}$	2.90	1.89	4527	$3.61 \cdot 10^{-5}$	1.33	0.50	4816
$N = 1000$	$3.21 \cdot 10^{-5}$	1.92	1.56	8428	$3.39 \cdot 10^{-5}$	0.87	0.33	9562
$N = 4000$	$3.26 \cdot 10^{-5}$	0.92	0.71	29347	$3.25 \cdot 10^{-5}$	0.40	0.17	37845

	dSS (Case 2)				dSS (Case 3)			
	$\overline{E[\hat{\pi}_F]}$	$\hat{\delta}_{\hat{\pi}_F}$	$R$	$N_T$	$\overline{E[\hat{\pi}_F]}$	$\hat{\delta}_{\hat{\pi}_F}$	$R$	$N_T$
$N = 250$	$3.97 \cdot 10^{-5}$	2.95	0.66	1997	$4.14 \cdot 10^{-5}$	4.38	2.13	2605
$N = 500$	$3.74 \cdot 10^{-5}$	2.13	0.51	3843	$3.51 \cdot 10^{-5}$	2.96	1.88	5093
$N = 1000$	$3.47 \cdot 10^{-5}$	1.33	0.39	7473	$3.41 \cdot 10^{-5}$	2.08	1.58	10025
$N = 4000$	$3.29 \cdot 10^{-5}$	0.65	0.24	28868	$3.27 \cdot 10^{-5}$	0.96	0.75	39787

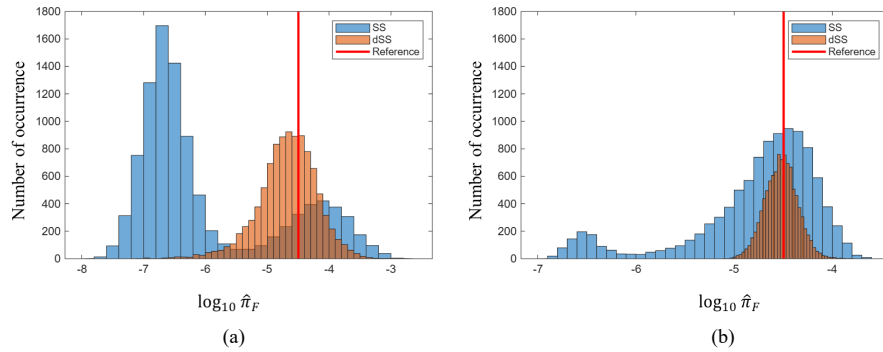


Fig. 3: Histogram of the  $\log_{10} \hat{\pi}_F$  estimates for the piecewise linear LSF in Example 4.1 obtained from  $10^4$  independent runs of the SS and Case 1 of the dSS methods, with (a)  $N = 500$  and (b)  $N = 4000$  samples per level and level probability of  $\rho = 0.2$ . The red line shows the reference value  $\log_{10} \hat{\pi}_{F,\text{ref}}$ .

is the root-mean square error of the failure probability estimates in the log-scale. Fig. 3 shows the histogram of the probability of failure estimates from  $m = 10^4$  independent runs. The results indicate superior performance of the dSS method in comparison to SS in Cases 1 and 2. Although the number of LSF evaluations in dSS is marginally higher, SS grossly underestimates the failure probability in majority of the runs, as depicted in Fig. 3. In contrast, the estimates from dSS have better concentration around the reference value. Consequently, the estimates from SS have significantly larger root-mean square error. Fig. 3 also depicts a smaller spread in the estimates from dSS, which leads to a smaller coefficient of variation. A comparison of  $\widehat{E}[\widehat{\pi}_F]$  with  $\widehat{\pi}_{F,\text{ref}}$  shows that the estimates from dSS have a slightly positive bias, which improves and becomes comparable to standard SS with increase in the per level sample size  $N$ . The performance of dSS, however, deteriorates in Case 3 and is indeed similar to SS. This is due to the poor choice of partition, where the main failure mode is located together with half of the smaller one in bin  $B_1$ .

The performance metric  $R$  is represented as a function of the average number of LSF evaluations  $N_T$  in Figure 4a.

## 4.2 Several beta points

In this example, we consider the LSF

$$g(\theta_1, \theta_2) = 12 - |\theta_1 \theta_2|, \quad (12)$$

where  $\theta_1$  and  $\theta_2$  are standard Gaussian random variables. Due to the symmetry of the LSF about the axes  $\theta_1 = 0$  and  $\theta_2 = 0$ , there are four failure modes with equal importance, as shown in Fig. 5. The reference value of the failure probability

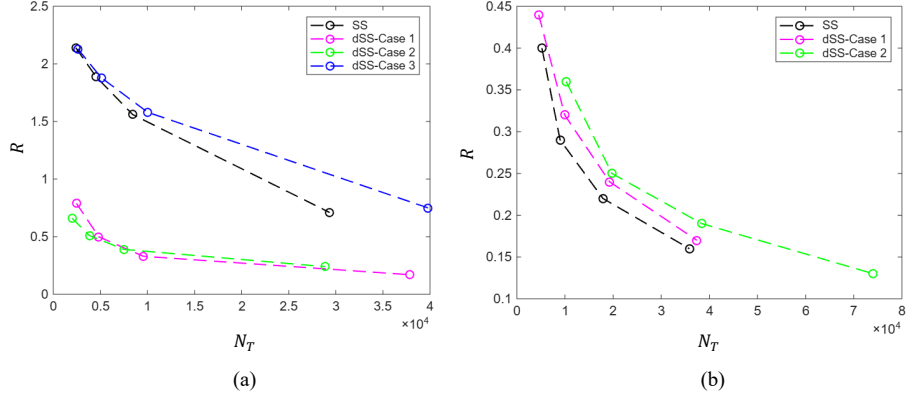
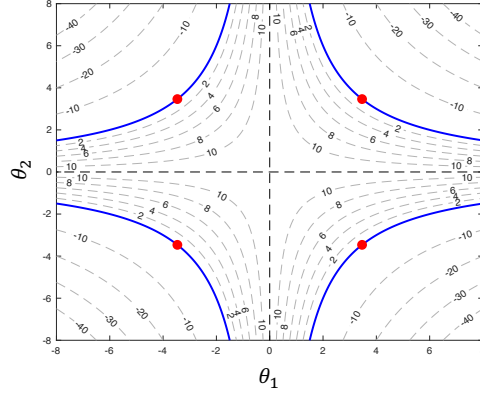


Fig. 4: Accuracy of the algorithms, as measured by the metric  $R$ , as a function of the average number of LSF evaluations  $N_T$ . Left: Example 4.1. Right: Example 4.2.

**Fig. 5** Contour plot of the LSF with several beta points in Example 4.2. The blue line denotes the boundary of the failure domain. The red dots are the four global design point, equidistant from the origin ( $\theta_1 = 0, \theta_2 = 0$ ).



obtained from brute-force Monte Carlo simulation with  $10^8$  LSF evaluations is  $\hat{\pi}_{F,\text{ref}} = 1.33 \cdot 10^{-6}$ .

Figs. 6 and 7 show the progression of samples in a typical run of the dSS and SS methods. To implement the dSS method, we consider two choice of partitions. In Case 1, we partition the parameter space into four bins of equal probability, which correspond to the four quadrants in the plane:

$$B_1 = \{\theta_1 \geq 0 \ \& \ \theta_2 \geq 0\}, \quad B_2 = \{\theta_1 \leq 0 \ \& \ \theta_2 \geq 0\}, \\ B_3 = \{\theta_1 \leq 0 \ \& \ \theta_2 \leq 0\}, \quad B_4 = \{\theta_1 \geq 0 \ \& \ \theta_2 \leq 0\}.$$

In Case 2, we consider a partition of eight equal bins, with each bin representing one half of the four quadrants. We see that SS fails to propagate the samples towards all the four failure modes, but with dSS all modes are explored.

A quantitative comparison of the performance of the two methods based on  $10^4$  independent runs is reported in Table 2. In contrast to Example 4.1, inadequacy in exploring the entire failure domain does not cause SS to underestimate the failure probability, because all the failure modes in this example have equal importance. The superior performance of dSS in exploring all the failure modes comes at the expense of reduced performance in estimating the global failure probability as indicated by comparatively higher values of  $\hat{\delta}_{\hat{\pi}_F}$  and  $R$ , particularly in Case 2. This is due to the requirement to estimate multiple local thresholds, four in Case 1 and eight in Case 2, with the same per level sample size  $N$ . However, this could be a reasonable trade-off in situations where it is important to be able to identify all the failure modes, and to assess the contribution of the individual modes to the global failure probability.

The performance metric  $R$  is represented as a function of the average number of LSF evaluations  $N_T$  in Figure 4.

Table 2: Probability of failure estimates for the LSF with several beta points in Example 4.2, obtained from  $m = 10^4$  independent runs of each algorithm. The reference value of the failure probability obtained from brute-force Monte Carlo simulation with  $10^8$  LSF evaluations is  $\hat{\pi}_{F,\text{ref}} = 1.33 \cdot 10^{-6}$ .

	SS				dSS (Case 1)			
	$\overline{E[\hat{\pi}_F]}$	$\hat{\delta}_{\hat{\pi}_F}$	$R$	$N_T$	$\overline{E[\hat{\pi}_F]}$	$\hat{\delta}_{\hat{\pi}_F}$	$R$	$N_T$
$N = 500$	$1.52 \cdot 10^{-6}$	2.76	0.40	5213	$2.12 \cdot 10^{-6}$	3.97	0.44	4552
$N = 1000$	$1.44 \cdot 10^{-6}$	1.02	0.29	8996	$1.69 \cdot 10^{-6}$	1.45	0.32	9944
$N = 2000$	$1.41 \cdot 10^{-6}$	0.86	0.22	17903	$1.56 \cdot 10^{-6}$	0.91	0.24	19280
$N = 4000$	$1.38 \cdot 10^{-6}$	0.49	0.16	35855	$1.46 \cdot 10^{-6}$	0.59	0.17	37394

	dSS (Case 2)				
	$\overline{E[\hat{\pi}_F]}$	$\hat{\delta}_{\hat{\pi}_F}$	$R$	$N_T$	
$N = 1000$	$2.18 \cdot 10^{-6}$	2.47	0.36	10249	
$N = 2000$	$1.73 \cdot 10^{-6}$	1.36	0.25	19749	
$N = 4000$	$1.56 \cdot 10^{-6}$	0.73	0.19	38411	
$N = 8000$	$1.46 \cdot 10^{-6}$	0.39	0.13	74025	

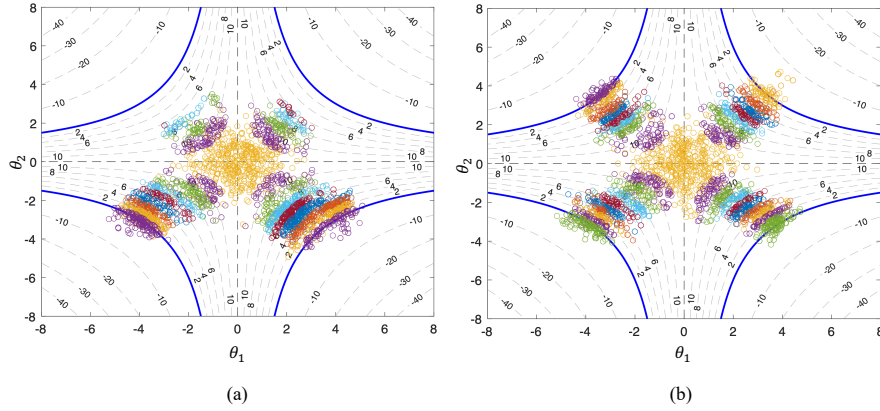
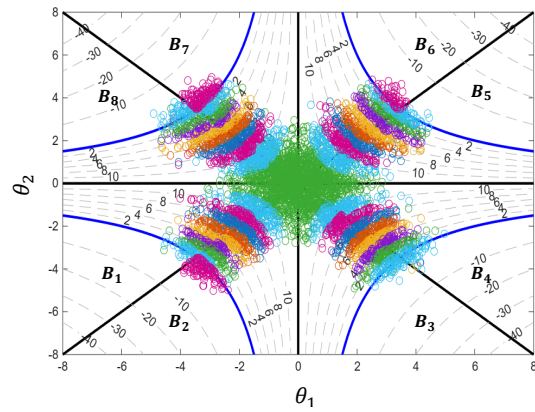


Fig. 6: Progression of samples in a typical run of (a) SS and (b) Case 1 of the dSS methods for the LSF with several beta points in Example 4.2, with  $N = 500$  samples per level and level probability of  $\rho = 0.2$ .

**Fig. 7** Progression of samples in a typical run of Case 2 of the dSS method for the LSF with several beta points in Example 4.2, with  $N = 2000$  samples per level and level probability of  $\rho = 0.2$ .



## 5 Conclusions

We propose a new advanced Monte Carlo method called directional subset simulation (dSS) to estimate small failure probabilities. dSS is an enhancement of the standard SS method for reliability analysis. It retains the generic multi-level nature of SS, wherein the small failure probability is estimated as a product of larger conditional probabilities of a nested sequence of intermediate failure events, or subsets, defined over the parameter space. However, the construction of the subsets in dSS differs from that in SS.

dSS works by partitioning the parameter space into non-overlapping bins. At each level, the global subset over the parameter space is a union of local subsets within each bin, defined in terms of a local threshold parameter that is estimated from the LSF values of the samples in the bin. As in SS, global MCMC moves are used to propagate samples from one level to the next. Numerical examples demonstrate that the use of multiple threshold parameters at each level provides an effective means to account for sudden sharp changes in the gradient of the LSF in different directions, which is an advantage over standard SS. It also facilitates adequate exploration of failure domains with multiple modes lying in different directions over the parameter space.

The choice of bins influences the performance of the dSS method. In many real-life engineering systems, experts are likely to have a prior idea of the failure modes of the system. This knowledge, when it is available, can be used to select the bins. When such knowledge is not available, the situation is more difficult. The naive “default” choice of using orthants results in very large number of bins if the input dimension large, which is a problem since each bin has its own local threshold that must be estimated.

A possible approach to address this issue is to develop an adaptive mechanism that automatically creates the bins as the algorithm progresses. One possibility is to start with a single run of standard SS, i.e., a single bin encompassing the parameter space, and use a suitable diagnostic measure to detect multimodality in the failure domain. In this context, unsupervised learning techniques such as clustering based on the LSF

values of the samples in each conditional level can be applied to detect the important directions containing the failure modes, and accordingly split the parameter space to create the bins. Future research will focus on incorporating the above ideas into the current framework of the dSS method. Another direction for future work is to compare the dSS method with other variants of SS, such as [19, 18, 9].

## Acknowledgment

The author O. Kanjilal acknowledges the German Academic Exchange Service (DAAD) for support through the Short-term Postdoc Grant (No. 57611805), and the Nemetschek Innovation Foundation for support through the TUM-GNI Postdoc Program.

## References

- [1] S. K. Au and J. L. Beck. Estimation of small failure probabilities in high dimensions by subset simulation. *Probabilistic Engineering Mechanics*, 16(4): 263–277, 2001.
- [2] K. Breitung. 40 years FORM: Some new aspects? *Probabilistic Engineering Mechanics*, 42:71–77, 2015.
- [3] K. Breitung. The geometry of limit state function graphs and subset simulation: Counterexamples. *Reliability Engineering & System Safety*, 182:98–106, 2019.
- [4] F. Cérou, P. Del Moral, T. Furon, and A. Guyader. Sequential Monte Carlo for rare event estimation. *Statistics and Computing*, 22:795–808, 2012.
- [5] O. Ditlevsen, R. E. Melchers, and H. Gluwer. General multi-dimensional probability integration by directional simulation. *Computers & Structures*, 36(2): 355–368, 1990.
- [6] R. Douc and O. Cappé. Comparison of resampling schemes for particle filtering. In *ISPA 2005. Proceedings of the 4th International Symposium on Image and Signal Processing and Analysis, 2005*, pages 64–69, 2005.
- [7] W. R. Gilks, S. Richardson, and D. J. Spiegelhalter. *Markov chain Monte Carlo in practice*. Chapman and Hall/CRC, 1996.
- [8] O. Kanjilal and C. S. Manohar. Markov chain splitting methods in structural reliability integral estimation. *Probabilistic Engineering Mechanics*, 40:42–51, 2015.
- [9] H. J. Kinnear and F. A. DiazDelaO. Niching subset simulation. *Probabilistic Engineering Mechanics*, 79:103729, 2025.
- [10] A. Der Kiureghian and T. Dakessian. Multiple design points in first and second-order reliability. *Structural Safety*, 20:37–49, 1998.
- [11] N. Kurtz and J. Song. Cross-entropy-based adaptive importance sampling using Gaussian mixture. *Structural Safety*, 42:35–44, 2013.

- [12] R. E. Melchers and A. T. Beck. *Structural reliability analysis and prediction*. John Wiley & Sons, 2018.
- [13] J. Nie and B. R. Ellingwood. A new directional simulation method for system reliability. Part I: application of deterministic point sets. *Probabilistic Engineering Mechanics*, 19:425–436, 2004.
- [14] I. Papaioannou and D. Straub. Combination line sampling for structural reliability analysis. *Structural Safety*, 88:102025, 2021.
- [15] I. Papaioannou, W. Betz, K. Zwirgmaier, and D. Straub. MCMC algorithms for subset simulation. *Probabilistic Engineering Mechanics*, 41:89–103, 2015.
- [16] I. Papaioannou, C. Papadimitriou, and D. Straub. Sequential importance sampling for structural reliability analysis. *Structural Safety*, 62:66–75, 2016.
- [17] H. J. Pradlwarter, G. I. Schuëller, P. S. Koutsourelakis, and D. C. Charnpis. Application of line sampling simulation method to reliability benchmark problems. *Structural Safety*, 29(3):208–221, 2007.
- [18] M. Rakshi. SESC: A new subset simulation method for rare-events estimation. *Mechanical Systems and Signal Processing*, 150(107139), 2021.
- [19] A. Sharma and C. S. Manohar. Modified replica exchange-based MCMC algorithm for estimation of structural reliability based on particle splitting method. *Probabilistic Engineering Mechanics*, 72:103448, 2023.
- [20] C. Song and R. Kawai. Monte Carlo and variance reduction methods for structural reliability analysis: A comprehensive review. *Probabilistic Engineering Mechanics*, 73:103479, 2023.
- [21] A. Tabandeh, G. Jia, and P. Gardoni. A review and assessment of importance sampling methods for reliability analysis. *Structural Safety*, 97:102216, 2022.
- [22] J. Xian and Z. Wang. Relaxation-based importance sampling for structural reliability ana. *Structural Safety*, 106:102393, 2024.
- [23] A. Zhang, Z. Chen, Q. Pan, X. Li, P. Feng, X. Gan, G. Chen, and L. Gao. Reliability analysis method for multiple failure modes with overlapping failure domains. *Probabilistic Engineering Mechanics*, 79:103741, 2025.
- [24] X. Zhang, Z. Lu, and K. Cheng. Cross-entropy-based directional importance sampling with von Mises-Fisher mixture model for reliability analysis. *Reliability Engineering & System Safety*, 220:108306, 2022.
- [25] K. M. Zuev, J. L. Beck, S. K. Au, and L. S. Katafygiotis. Bayesian post-processor and other enhancements of subset simulation for estimating failure probabilities in high dimensions. *Computers & Structures*, 92–93:283–296, 2012.